ASCE

Risk-Based Design of Regular Plane Frames Subject to Damage by Abnormal Events: A Conceptual Study

André T. Beck[1]; Lucas da Rosa Ribeiro[2]; Marcos Valdebenito[3]; and Hector Jensen[4]

Abstract: Constructed facilities should be robust with respect to the loss of load-bearing elements due to abnormal events. Yet, strengthening structures to withstand such damage has a significant impact on construction costs. Strengthening costs should be justified by the threat and should result in smaller expected costs of progressive collapse. In regular frame structures, beams and columns compete for the strengthening budget. In this paper, we present a risk-based formulation to address the optimal design of regular plane frames under element loss conditions. We address the threat probabilities for which strengthening has better cost-benefit than usual design, for different frame configurations, and study the impacts of strengthening extent and cost. The risk-based optimization reveals optimum points of compromise between competing failure modes: local bending of beams, local crushing of columns, and global pancake collapse, for frames of different aspect ratios. The conceptual study is based on a simple analytical model for progressive collapse, but it provides relevant insight for the design and strengthening of real structures. **DOI: 10.1061/(ASCE)ST.1943-541X.0003196.**

Author keywords: Risk optimization; Progressive collapse; Alternative path method; Discretionary column removal; Structural reliability; Regular frame structures; Optimal design; Probability threshold.

Introduction

Modern structural engineering requires built structures to be robust with respect to damage caused by abnormal events of exceptionally large intensity but low probability of occurrence. Following the recent partial or full collapses of buildings like Ronan Point Tower, Skyline Plaza, Alfred P. Murrah, and the World Trade Center, design requirements for structural robustness were introduced in modern design codes [ASCE 7 (ASCE 2016); ASCE 41 (ASCE 2017); DoD 2013; GSA 2013]. The design of robust structures is achieved by analyzing progressive collapse under potential initial damage.

Under multiple hazards, the probability of structural collapse can be evaluated as (Ellingwood and Dusenberry 2005; Ellingwood 2006, 2007)

$$p_C = P[C] = \sum_H \sum_{LD} P[C|LD,H]P[LD|H]P[H] \quad (1)$$

where C = collapse; $P[H]$ = probability of hazard occurrence; $P[LD|H]$ = conditional probability of local damage, given hazard H; and $P[C|LD,H]$ = conditional probability of collapse, given local damage LD and hazard H. In Eq. (1), the sum over H indicates the multiple hazards the structure is exposed to (for example, loads due to vehicular collisions, explosion, fire, and terrorist attacks), and the sum over LD represents the different initial damage states the structure can experience (e.g., local damage, support subsidence, internal or external column loss, and penultimate column loss).

Some terms in Eq. (1) depend on structural mechanics, while others depend on human, social, and political factors. A risk analysis of the structure, considering its surrounding environment and intended use, can address control of the hazards or reduction of their rates of occurrence ($P[H]$). To some extent, protective measures arising from risk analysis can limit local damage produced by hazard H (term $P[LD|H]$). Structural mechanics controls the terms $P[LD|H]$ and $P[C|LD,H]$; this last related to damage propagation following initial damage. Threat-independent approaches to robust design assume that local damage will occur, with loss of load-bearing elements, and focus on the damage propagation term.

The damage propagation analysis can be made independent of the nonstructural (social, environmental, political) factors by considering initial damage probability as an independent parameter, following Beck (2020) and Beck et al. (2020)

$$p_{LD} = \sum_H P[LD|H]P[H] \quad (2)$$

where p_{LD} = probability of local damage, like loss of a column, loss of a load-bearing wall, and loss of a support.

In this paper, we study the progressive collapse of regular frame structures subject to initial damage, like loss of columns and adjacent beams. A regular frame is understood as one with the same bay length over height, and the same height for all floors. Specifically, we address the optimal design of regular frame buildings, considering the impacts of initial damage due to abnormal events. We employ the formulation of Beck et al. (2020), which considers the usual loading condition as one of the "hazards" in Eq. (1), with unitary probability of occurrence. The risk-based formulation looks for the minimum total expected costs of the building structure,

[1]Associate Professor, Dept. of Structural Engineering, Univ. of São Paulo, Av. Trabalhador São-carlense, 400, São Carlos, SP 13566-590, Brazil (corresponding author). ORCID: https://orcid.org/0000-0003-4127-5337. Email: atbeck@sc.usp.br

[2]Ph.D. Student, Dept. of Structural Engineering, Univ. of São Paulo, Av. Trabalhador São-carlense, 400, São Carlos, SP 13566-590, Brazil. ORCID: https://orcid.org/0000-0002-5705-9957. Email: lucasribeiro@usp.br

[3]Professor, Faculty of Engineering and Sciences, Universidad Adolfo Ibáñez, Av. Padre Hurtado 750, Viña del Mar 2562340, Chile. Email: marcos.valdebenito.castillo@gmail.com

[4]Professor, Departmento de Obras Civiles, Universidad Tecnica Federico Santa Maria, Av. España 1680, Valparaíso 110V, Chile. Email: hector.jensen@usm.cl

Note. This manuscript was submitted on February 10, 2021; approved on July 27, 2021; published online on October 19, 2021. Discussion period open until March 19, 2022; separate discussions must be submitted for individual papers. This paper is part of the ***Journal of Structural Engineering***, © ASCE, ISSN 0733-9445.

which includes construction costs ($C_{constr.}$), cost of strengthening the frame to produce alternative load paths, cost of initial damage (C_{LD}), and eventual costs due to damage propagation ($C_{DP|LD}$) and/or collapse due to damage propagation ($C_{C|LD}$), where subscript $(\cdot)_{DP}$ is for damage propagation. The design variables are the design factors for beams (λ_B) and columns (λ_C). With these terms, the risk-optimization problem is stated as (Beck and de Santana Gomes 2012; Beck et al. 2015, 2019)

$$\begin{aligned} \text{Find: } & \{\lambda_B^*, \lambda_C^*\} \\ \text{which minimizes: } & C_{TE}(\lambda_B, \lambda_C) = C_{constr.} + p_{LD}(C_{LD} + p_{DP|LD}C_{DP|LD} + p_{C|LD}C_{C|LD}) + p_f C_{NLC} \\ \text{subject to: } & \lambda_B, \lambda_C > 0 \end{aligned} \tag{3}$$

In Eq. (3), p_f = probability of failure under normal loading conditions; and C_{NLC} = corresponding cost of failure term. This last term is considered mainly to cover the cases where p_{LD} is very small, following Beck et al. (2020). Note that the probability of local damage p_{LD} in Eq. (3) is the lifetime (herein, 50-year) probability. This can be related to yearly threat probabilities by $p = -\ell n[1 - p_{LD}]/50$.

The damage propagation and collapse terms in Eq. (3) depend on local failure of beams, local failure of columns adjacent to the initial damage, and global failure of columns (pancake failure). These probability and cost terms are described later in the paper.

In this paper, we investigate optimal designs resulting from Eq. (3) when applied to regular plane frames of varying aspect ratios, extents of initial damage, strengthening decisions, and other factors. The analysis is a significant extension of results presented in Beck et al. (2020, 2021). In particular, herein we address the competition between local bending, local crushing, and global pancake failure modes for frames of varying aspect ratios. In this paper, we do not address practical design aspects such as binding, structural fuses, compressive arch, and Vierendeel actions. We employ a simple analytical model for the progressive collapse that considers the plastic bending collapse of beams and the crushing collapse of columns. The model is limited to plane frames and to gravitational loads. Results provide insight that can be useful for actual structural design but which needs to be verified using more complete models (Gerasimidis and Sideri 2016; Pantidis and Gerasimidis 2018) and specialized software (Adam et al. 2018).

One important aspect of design for robustness is the threat probability that justifies strengthening structural elements to provide alternative load paths, for instance. Addressing this issue, Beck et al. (2020) introduced the concept of a *threshold column loss probability*. Herein, we address local initial damage of different magnitude, potentially affecting a larger number of columns; also beams and slabs. Therefore, we recall the concept by giving it a more general name:

"*Local damage* probability threshold p_{LD}^{th} is the value above which design for alternative (load) paths under discretionary local damage has positive cost-benefit, in comparison to usual design."

In this paper, we make an extensive investigation of how the p_{LD}^{th} value changes for frames of varying aspect ratios for different extents of initial damage and strengthening decisions.

The remainder of this paper is organized as follows. The mechanical model for damage propagation and collapse of regular frames under gravity loads is presented in the "Progressive Collapse of Regular Plane Frames: Mechanical Model" section. Formulation of the cost functions for risk-based optimization is presented in the "Formulation of the Cost-Benefit Risk-Optimization Problem" section. Numerical results are presented in the "Results for the Reference Case" section for a reference frame case and in the "Results for Other Frame Configurations" section for several variants. Conclusions are presented in the "Concluding Remarks" section.

Progressive Collapse of Regular Plane Frames: Mechanical Model

Basic Formulation

This paper addresses the design and strengthening of regular two-dimensional multistory multibay frames, as illustrated in Fig. 1. The mechanical model for damage propagation and progressive collapse, under gravity loads and initial damage, is based on Masoero et al. (2013). The model targets steel or reinforced concrete (RC) frames and considers the bending failure of beams and the crushing failure of columns. The model considers regular frames with n_c columns and n_s stories and an initial damage event

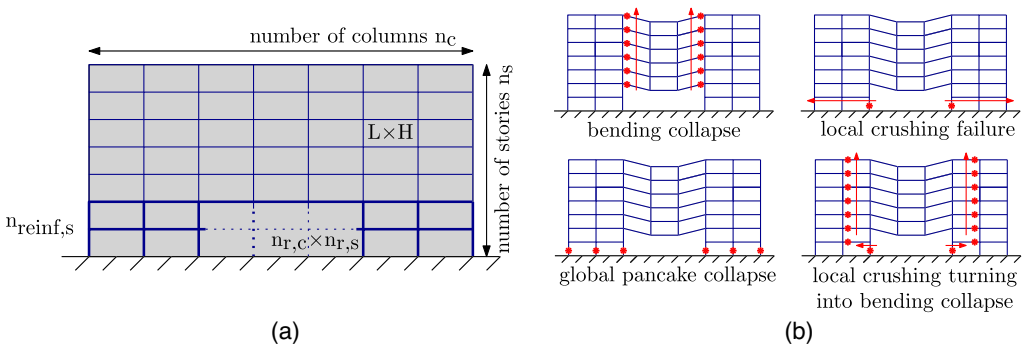

Fig. 1. (a) Sketch of the regular plane frame; and (b) collapse mechanisms.

J. Struct. Eng., 2022, 148(1): 04021229

leading to failure of $n_{r,c}$ columns and $n_{r,s}$ stories, where the subscript r is for removed. Here, $n_{r,s}$ refers to the vertical extent of the initial damage [Fig. 1(a)]. Beam length is L for all spans, and column height is H for all stories.

The simple analytical model of Masoero et al. (2013) has a few acknowledged limitations, which should be considered when interpreting results in this paper:

1. The model is limited to gravitational loads: wind, earthquake, and other lateral loads are not considered; out-of-plumbness is not considered,
2. As a plane model, floor and other three-dimensional effects are ignored. Neglecting floor effects may underestimate the resistance significantly (He et al. 2019),
3. Compressive arching effects significantly increase the resistance to progressive collapse but are not considered in the model, and
4. Strength and failure of beam-column connections are not considered.

Albeit simple, the model is useful for a conceptual cost-benefit analysis of design against progressive collapse. With removal of $n_{r,c}$ columns of $n_{r,s}$ stories, the frame may suffer bending collapse of $n_{r,c}+1$ bays, or local crushing failure of two adjacent columns, as illustrated in Fig. 1(b). Local crushing may propagate horizontally, leading to bending collapse of $n_{r,c}+3$ bays, and so on, eventually extending the full horizontal extent of the frame, leading to global pancake collapse.

In the following, superscript I is employed for the intact structures. Superscripts B and P refer to bending and pancake collapse. Pancake collapse can be local (P, loc) or global (P, gl). Furthermore, perfect brittleness is denoted el, whereas ideal plastic behavior is written as pl. This notation follows Masoero et al. (2013) for easy cross-referencing. The whole formulation is presented in terms of distributed loads q_u. The plastic hinge moment for beams is B_y, and crushing strength of columns is R_c.

For the intact structure, the ultimate strength in bending collapse is obtained as

$$q_u^{I,B,pl} = \frac{16B_y}{L^2} \tag{4}$$

This plastic solution is derived from the kinematic theorem, considering a triple-hinge plastic mechanism. In case of damage to $n_{r,c}$ columns, bending collapse strength is given by

$$q_c^{B,pl}(n_{r,c}) = \frac{4B_y}{L^2(n_{r,c})} \tag{5}$$

For the intact structure, static crushing of the columns occurs when maximum compressive force at base equals total axial strength, leading to the global pancake collapse strength

$$q_u^{I,P} = \frac{R_c}{Ln_s}\frac{n_c}{(n_c-1)} \tag{6}$$

In case of local damage, local and global pancake collapses are possible. In the case of local pancake, overload is directed to the two nearest intact columns. Brittle failure occurs for

$$q_c^{P,loc,el}(n_{r,c}, n_{r,s}) = \frac{R_c}{Ln_s}\frac{1}{(2-\frac{n_c-1}{n_c}+n_{r,c}(1-\frac{n_{r,s}}{n_s}))} \tag{7}$$

In case of damage to $n_{r,c}$ columns, brittle global pancake collapse occurs for

$$q_c^{P,gl,el}(n_{r,c}, n_{r,s}) = \frac{R_c}{Ln_s}\frac{n_c(n_c-n_{r,c})}{((n_c-1)(n_c+n_{r,c})-2\frac{n_{r,s}}{n_s}n_{r,c}n_c)} \tag{8}$$

In our implementation, we consider the ductile failure of beams and the brittle elastic failure of columns. Hence, our analysis is representative of RC frame buildings. Following the developments of Masoero et al. (2013), the dynamic load amplification factor is $DAF = 1$ for beams and $DAF = 2$ for columns. This is closely related to the recommended DAF values for deformation-controlled plastic failure of beams, and load-controlled failure of columns (GSA 2013).

Reference Case

Several frame and initial damage configurations are studied, as detailed later in the paper. In order to organize comparisons, a so-called *reference* case is initially considered: a frame with eight stories and eight bays $(n_s \times (n_c-1) = 8\times 8)$, with beam length $L = 2H = 6$ m. This frame is initially designed considering normal loading conditions and later strengthened considering discretionary removal of a single column and two adjacent beams from one bay $(n_{r,c}^0 = 1, n_{r,s}^0 = 1)$. The superscript $(\cdot)^0$ refers to the initial discretionary damage for which the frame is strengthened.

The reference value for the probability of local damage is $p_{LD} = 0.1$, as detailed later. This 50-year probability corresponds to an annual threat probability of 2.1×10^{-3}. Risk-optimization results are computed for $10^{-6} \le p_{LD} \le 1$.

Design under Normal Loading Condition

In the following, numerical results are presented for the *reference* frame configuration. The nominal dead and live loads are $L_n = D_n = 1(\text{kN/m})$. Under normal loading conditions, the required beam strength is [ASCE 7 (ASCE 2016)]:

$$B_y^{NLC} = \frac{L^2}{16\phi}q_u^{I,B,pl} = \frac{L^2}{16\phi}(1.2D_n+1.6L_n) = 7.41 \text{ kN}\cdot\text{m} \tag{9}$$

Superscript $(\cdot)^{NLC}$ refers to the normal loading condition. The required column strength is

$$R_c^{NLC} = \frac{Ln_s(n_c-1)}{\phi n_c}q_u^{I,P} = \frac{Ln_s(n_c-1)}{\phi n_c} = (1.2D_n+1.6L_n) = 140.55 \text{ kN} \tag{10}$$

In Eqs. (9) and (10), $\phi = 0.85$ is employed herein to design the RC frame. Note that, for design of compression-controlled elements like columns [Eq. (10)], the design factor would be 0.85/0.65 = 1.3 larger. This should be taken into account when interpreting optimal design factors for columns found herein. In the remainder of this text, the frame designed under normal loading conditions is referred to as the *normal* frame.

Strengthening under Initial Damage Condition

In the following, numerical results are presented for the reference case, where strengthening is considered for one column and two beams removed from one floor. Yet, it is assumed that any column of the first floor could be lost; hence, all columns and all beams of the first two floors need to be strengthened. The superscript $(\cdot)^0$ refers to the initial damage, for which the frames are strengthened. This is to distinguish from progressive failure involving damage to $n_{r,c}$ columns.

Beams and columns are strengthened in such a way as to provide an alternative path to the loads supported by the removed elements (Alternate Path Method, GSA 2013). For the beams to bridge over a single removed column, the required bending strength is [ASCE 7 (ASCE 2016)]

$$B_y^0(n_{r,c}^0 = 1) = \frac{L^2(n_{r,c}^0)}{4\phi} q_c^{B,pl} = \frac{L^2}{4\phi}(1.2D_n + 0.5L_n)$$
$$= 15.3 \text{ kN} \cdot \text{m} \quad (11)$$

Considering load redistribution, the required strength for adjacent columns is

$$R_c^0(n_{r,c}^0, n_{r,s}^0)$$
$$= Max\left[R_c^{NLC}, \frac{Ln_s}{\phi}\left(2 - \frac{n_c - 1}{n_c} + n_{r,c}^0\left(1 - \frac{n_{r,s}^0}{n_s}\right)\right) q_c^{P,loc,el}\right]$$
$$= 162.1 \text{ kN} \quad (12)$$

with $q_c^{P,loc,el} = (1.2D_n + 0.5L_n) = 1.7$ kN/m. In strengthening, we consider $\phi = 1$, as recommended in ASCE 41 (ASCE 2017). In Eq. (12), operator $Max[]$ is used to also consider the required column strength under normal loading condition. This operator is not required in Eq. (11) because the impact of a lost column in bending moments is large for $L \geq H$. The resulting strengthening factors $(\cdot)_{sf}$ for beams and columns are

$$B_{sf} = B_y^0(n_{r,c}^0)/B_y^{NLC} = 2.06 \quad \text{and}$$
$$R_{sf} = R_c^0(n_{r,c}^0, n_{r,s}^0)/R_c^{NLC} = 1.23 \quad (13)$$

In order to address optimal design under an initial damage condition, we use independent design factors for beams (λ_B) and columns (λ_C). These are in addition to the usual code-recommended factors, such that $\lambda_B = \lambda_C = 1$ recovers the code-recommended design [ASCE 7 (ASCE 2016); ASCE 41 (ASCE 2017)]. Hence, strength equations [Eqs. (4)–(8)] are computed with B_y replaced by $B_y = \lambda_B B_y^0$, and with R_c replaced by $R_c = \lambda_C R_c^0$, where B_y^0 and R_c^0 are the initial values of beam plastic hinge moment and column crushing capacities, respectively. In the remainder of this text, the frame designed under discretionary initial damage is referred to as the *strengthened* frame. Strengthening two floors of the reference frame, has an impact of 13% on total construction costs, as detailed later.

Limit States and Reliability Analysis

The risk-based cost-benefit analysis addressed herein combines failure of the intact structure with failure/progressive collapse under initial damage conditions. For the intact structure, the limit state function for bending and global pancake collapse is

$$g_I(\lambda_B, \lambda_C, \mathbf{X}) = R_I r_I(\lambda_B, \lambda_C, \cdots) - D - L_{50} \quad (14)$$

where $r_I(\cdot)$ = deterministic strength function for the intact structure; R_I = nondimensional random variable describing uncertainty in the strength of the intact structure, including model error; D = dead load; L_{50} = 50-year extreme live load; and $\mathbf{X}$ = vector of random system parameters. Usually, Eq. (14) is not a function of the progressive collapse design factors λ_B and λ_C. However, as the structural elements are strengthened for load bridging under discretionary element removal, the reliability index for normal loading conditions also becomes a function of λ_B and λ_C. The strength function $r_I(\cdot)$ for bending failure is given by Eq. (4) and for global pancake by Eq. (6).

In case of localized initial damage, the limit state function is given by

$$g_{LD}(\lambda_B, \lambda_C, \mathbf{X}) = R_D r_D(\lambda_B, \lambda_C, n_{r,c}, n_{r,s} \ldots) - D - L_{apt} \quad (15)$$

where $r_D(\cdot)$ = deterministic strength function for the damaged structure; R_D = nondimensional random variable describing uncertainty in the strength of the damaged structure, including model error; and L_{apt} = sustained component of live load. In Eq. (15), the strength function $r_D(\cdot)$ for bending is Eq. (5), for local crushing is Eq. (7), and for global pancake failure is Eq. (8). Note that these equations are valid for any number of removed columns ($n_{r,c} < n_c$). This includes the initial triggering event as well as the progressive failure of columns.

By treating beam and column strength as the product of deterministic functions (r_I and r_D) by single random variables (R_I and R_D), the limit state functions become linear, allowing a second-moment solution. Statistics for R_I and R_D are different for the beam and columns, as illustrated in Table 1. The statistics for these variables reflect material variability and model error and were obtained by simulation from data in Nowak et al. (2011). Data on random variables R_I and R_D should be reviewed in more practical applications, especially when considering horizontal loads and other failure models.

By approximating the probability distributions of L_{apt} and L_{50} as Gaussian, the limit state functions become linear functions of Gaussian variables, and reliability can be computed by the Cornell reliability index (Melchers and Beck 2018). This is considered accurate enough for the conceptual problem addressed herein. For more practical applications, the use of FORM or Monte Carlo simulation is recommended (Ang and Tang 2006; Melchers and Beck 2018).

For an intact frame, the 50-year Cornell reliability index is

$$\beta^{50}(\lambda_B, \lambda_C) = \frac{r_I(\lambda_B, \lambda_C)\mu_{R_I} - (\mu_D + \mu_{L_{50}})}{\sqrt{r_I(\lambda_B, \lambda_C)^2 \sigma_{R_I}^2 + (\sigma_D^2 + \sigma_{L_{50}}^2)}} \quad (16)$$

where μ = mean; and σ = standard deviation of the corresponding variables. The reliability index for bending collapse of the intact frame is obtained for $r_I(\lambda_B) = q_u^{I,B,pl}$ [Eq. (4)], with $B_y = \lambda_B B_y^0$; for global pancake collapse, β^{50} is computed with $r_I(\lambda_C) = q_u^{I,P}$ [Eq. (6)], with $R_c = \lambda_C R_c^0$.

Table 1. Random variable statistics

Variable	Mean (μ)	COV (σ/μ)	Distribution	References
Plastic moment strength, bending of RC beams/slabs (R_{BS})	1.22	0.165	Normal	Beck et al. (2020), based on Nowak et al. (2011).
Crushing strength of RC columns (R_C)	1.20	0.184	Normal	Beck et al. (2020), based on Nowak et al. (2011).
Dead load (D)	$1.05D_n$	0.10	Normal	Ellingwood et al. (1980), and Ellingwood and Galambos (1982).
Live load, arbitrary point in time value (L_{apt})	$0.25L_n$	0.55	Gamma	Ellingwood et al. (1980), and Ellingwood and Galambos (1982).
Live load, 50 years (L_{50})	$1.0L_n$	0.25	Gumbel	Ellingwood et al. (1980), and Ellingwood and Galambos (1982).

Table 2. Reliability index values for *reference* frame

		Intact frame:		Conditional on initial damage:	
β	Failure mode	NLC	Strengthened	Damaged	Optimized
β^{apt}	Global pancake	3.56	3.82	**3.46**	**3.93**
	Local pancake	—	—	**1.80**	**2.62**
	Bending	3.99	5.10	**2.03**	**1.61**
	Catenary ($\psi = 2$)	4.42	5.31	**3.36**	**1.81**
β^{50}	Global pancake	**2.46**	**2.85**	2.30	3.03
	Local pancake	—	—	−0.02	1.08
	Bending	**2.76**	**4.50**	0.06	−0.45
	Catenary ($\psi = 2$)	**3.43**	**4.83**	1.84	−0.21

Note: Numbers presented in bold values are those that are usually computed; other numbers are presented for completeness.

Given local initial damage, the conditional arbitrary-point-in-time (*apt*) reliability index is

$$\beta = \beta^{apt}(\lambda_B, \lambda_C, n_{r,c}, n_{r,s}) = \frac{r_D(\lambda_B, \lambda_C, n_{r,c}, n_{r,s})\mu_{R_D} - (\mu_D + \mu_{L_{apt}})}{\sqrt{r_D(\lambda_B, \lambda_C, n_{r,c}, n_{r,s})^2\sigma^2_{R_D} + (\sigma^2_D + \sigma^2_{L_{apt}})}} \quad (17)$$

The reliability indexes for bending collapse (β_B), local pancake (β_{PL}), and global pancake (β_{PG}) are obtained using Eqs. (5), (7), and (8), respectively. In the following, since we mainly refer to local damage conditions, the superscripts $(\cdot)^{50}$ and $(\cdot)^{apt}$ are dropped for clarity of notation, when there is no risk of confusion. Reliability indexes obtained for the initial design of the *reference* frame are presented in Table 2. Numbers presented in bold values are those that are not usually computed but which are presented here for completeness. Individual columns in Table 2 show how reliability changes along the design process: from the initial design, under normal loading conditions [Eqs. (9) and (10)], to strengthening using Eqs. (11) and (12) with $\lambda_B = \lambda_C = 1$, starting from the intact condition and moving to the conditional damage condition. The last column shows reliability indexes obtained from the risk optimization, as detailed in the sequence.

Formulation of the Cost-Benefit Risk-Optimization Problem

The decision to strengthen a structure, to make it able to bridge over a removed load-bearing element, has an obvious impact on construction costs. In order to investigate the cost-benefit of different strengthening decisions, in potential initial damage scenarios, the costs of strengthening have to be confronted with the costs of building the structure and the expected costs of failure. Costs of failure include the costs of initial damage, cost of damage propagation, and eventually, cost of full-frame collapse.

Construction Cost

In this paper, all cost terms are evaluated w.r.t. the cost for building the frame structure. Hence, the cost of the structural frame is the reference cost, C_{REF}. Costs of structural materials vary significantly with geographical location in terms of absolute values and in terms of the relative cost of steel to concrete. The cost of an RC structure, for instance, depends on the cost of reinforcing steel, cost of concrete, and cost of formwork and steel forming. These costs vary significantly due to, for example, geographical factors. As a simplification, and in benefit of generality, we assume unitary costs per length of beams and columns. For a span-to-height ratio of $L = 2H$ and for $L = 6$ m, the cost per meter of optimized beams and columns was found to be about the same by Boito and Kripka (2020). Hence, the reference cost is given by the total linear length of the frame

$$C_{REF} = Ln_s(n_c - 1) + Hn_sn_c \quad (18)$$

This is understood as the cost of designing the frame under normal loading conditions. If the frame is strengthened to bridge over failed elements, construction costs increase. Typically, design for progressive collapse is of secondary nature (He et al. 2019); hence, after the main elements are sized considering normal loading conditions [Eqs. (9) and (10)], they are verified under exceptional loading or element removal conditions and eventually strengthened. Typically, strengthening is done by increasing the steel reinforcement area. When a column fails under a multispan beam, maximum moments at the beam section above the column go from negative to positive. Hence, one immediate strengthening action is to use double (symmetric)instead of single reinforcement.

Considering typical ductile RC beams, we found that in order to double the strength of a beam in bending, it is required to roughly double the steel area. The impact in construction costs depends on the participation factor of steel to total costs, given as α_B for beams. Hence, the cost of strengthening the beams of each floor for bridging over $n^0_{r,c}$ removed columns is proportional to the following factor:

$$(\lambda_B\alpha_B B_{sf} + (1 - \alpha_B)) \quad (19)$$

Note that Eq. (19) includes the bending design factor λ_B. Using construction cost tables for Brazil (SINAPI 2020), we found that the participation of steel in the total construction costs of a beam is roughly 70%. Hence, our reference value is $\alpha_B = 0.7$, but other values are also considered later in the paper. In Eq. (19), $(1 - \alpha_B)$ is the fixed part of beam construction costs.

Using similar reasoning, the cost factor for strengthening frame columns is written as

$$(\lambda_C\alpha_C R_{sf} + (1 - \alpha_C)) \quad (20)$$

Finding the participation cost factor of columns is more difficult, as it strongly depends on concrete strength, load eccentricity, and other factors. Hence, in order to reduce the number of parameters in the analysis, we consider $\alpha_C = \alpha_B = \alpha = 0.7$ in the following, unless stated otherwise. These factors should be verified when addressing more practical problems.

To keep the presented cost terms in perspective, Praxedes and Yuan (2021, 2022) strengthened two four-story four-bay frames to bridge over the loss of a single internal column. Their strengthening action was to increase the steel ratio of about half the frames (covering beams and columns above two out of four bays). By comparing the construction cost of the strengthened frames with the cost of the original frames, we arrive at $0.3 \lesssim \alpha \lesssim 0.4$. If the whole frames were strengthened, one would obtain $0.6 \lesssim \alpha \lesssim 0.8$.

Another important strengthening decision refers to the number of columns and the number of beams to be strengthened. In a fully threat-independent design, all beams and columns should be strengthened. However, such a decision has a strong impact on construction costs and was shown not to be economical for typical threat probabilities (Beck et al. 2020; Praxedes 2020; Praxedes and Yuan 2021, 2022). For some threats like traffic accidents and explosions due to malevolent actions, first floor and building entrance columns are obvious targets. However, the extent of the initial

damage may not be limited to the first floor. Hence, in this paper, the reference strengthening action is to reinforce all columns and all beams of the first two floors. This goes in line with the findings of Praxedes and Yuan (2022) that optimal robustness is obtained when most reinforcement is allocated to the first floor, followed by the second floor.

In order to simplify notation, the unitary construction costs of beams and columns are written as

$$C_{beams}(\lambda_B, n_{reinf,s}) = \{n_s - n_{reinf,s} + n_{reinf,s}(\lambda_B \alpha_B B_{sf} + (1 - \alpha_B))\} \quad (21)$$

$$C_{columns}(\lambda_C, n_{reinf,s}) = \{n_s - n_{reinf,s} + n_{reinf,s}(\lambda_C \alpha_C R_{sf} + (1 - \alpha_C))\} \quad (22)$$

The presented terms include the original cost of construction, plus the cost of strengthening per unit length. The total construction cost is

$$C_{const.}(\lambda_B, \lambda_C) = \frac{1}{C_{REF}}[L(n_c - 1)C_{beams}(\lambda_B, n_{reinf,s}) + Hn_c C_{columns}(\lambda_C, n_{reinf,s})] \quad (23)$$

For usual design under normal loading conditions, the same cost functions are considered, but with no strengthening ($n_{reinf,s} = 0$).

Cost of Failure

For the conceptual study presented herein, the cost of failure is assumed proportional to the extent of the damaged frame area. For an initial damage event leading to loss of $n^0_{r,c}$ columns from $n^0_{r,s}$ floors, the cost of initial damage is

$$C_{ID} = \frac{1}{C_{REF}}(2Ln^0_{r,s} + Hn^0_{r,c}) \quad (24)$$

Failure consequences are strongly dependent on nonstructural factors, such as building surrounding environment and intended use. Consequences of structural failure involve the costs of shutdown for rehabilitation and repair (lost revenue), costs for removing debris and rebuilding, damage to building contents and neighboring facilities, injury, death, and environmental damage. Out of these, only the cost of reconstruction depends on design safety margins. Hence, to separate nonstructural consequence factors from the structural reliability analysis, as advocated in Beck (2020) and Beck et al. (2020, 2021), failure consequences are considered via an independent cost parameter k. Failure cost multipliers are a significant source of epistemic uncertainty, and they can change significantly for different structures, real estate market conditions, and economy interest rates (as failures occur in the future, w.r.t construction time).

The cost of construction in Eq. (23) is the cost of the structural frame. Marchand and Stevens (2015) studied ratios between the costs of entire buildings and construction costs of structural frames. These ratios were found to be 6.8 for RC frames, 16.7 for steel frames, 4.4 for cold-formed steel, and 10.5 for wood structures. Collapse failure costs are easily higher than the costs for reconstructing the whole building, and not just the structural frame. Hence, collapse failure cost multipliers can be significantly higher than the figures presented and should be considered constant instead of functions of λ_B and λ_C.

Financial losses from the partial collapse of the Alfred P. Murrah Federal Building were estimated at $652 million by Hewitt (2003). This eight-story RC building was built in 1977 at a cost of $14.5 million, or 24.7 million 1995 dollars at an annual interest of 3%, which yields a total loss to building cost ratio of 26.4. The partial collapse affected 42% of the floor area of the building; a full collapse could bring this figure up significantly. Total losses arising from the 9/11 WTC attacks were 40 times larger than the building cost (Stewart 2017; Thöns and Stewart 2020), whereas a factor of 20 was found for the Pentagon (Muller and Stewart 2011). In a cost-benefit analysis of terrorism risk-reduction measures for buildings, Stewart (2017) considered total loss to building cost ratios in the range 20–40. Considering these figures as a reference, herein we consider $k = 40$ as a base case and an upper-range value $k = 80$.

For engineering structures, brittle failures are usually more critical than ductile failures. Ductile failures provide warnings, allowing damaged structures to be evacuated, whereas brittle failures occur with little or no warning. When RC elements are properly designed, the bending failure of beam/slabs is mostly ductile. The simple model by Masoero et al. (2013) does not consider column slenderness, nor the bending-compression failure of columns. Since only axial load capacity is considered, we assume the crushing failure of columns to be brittle. To account for the different consequences of failure, the cost multiplier for brittle failure (local and global pancake collapse) is twice that of ductile failure: $k_{brittle} = 2k_{ductile} = 40$, unless otherwise stated.

Costs of local collapse failures by bending or pancake are given by the impacted frame area (total linear length) immediately above the removed or failed column, multiplied by failure cost multipliers k. The cost of bending collapse is computed as

$$C_B(n_{r,c}) = \frac{k_{ductile}}{C_{REF}}(Min[n_{r,c} + 1, n_c - 1]LC_{beams}(\lambda_B = 1) + Min[n_{r,c}, n_c]HC_{columns}(\lambda_C = 1)) \quad (25)$$

and the cost of local pancake collapse is computed as

$$C_{PL}(n_{r,c}) = \frac{k_{brittle}}{C_{REF}}(Min[n_{r,c} + 3, n_c - 1]LC_{beams}(\lambda_B = 1) + Min[n_{r,c} + 2, n_c]HC_{columns}(\lambda_C = 1)) \quad (26)$$

In Eqs. (25) and (26), the $Min[]$ operators warrant that costs of local collapse will not exceed costs of global collapse if local pancake progresses into global pancake collapse. The evolution of the cost of local failures, in terms of the number of removed columns, is illustrated in Fig. 12 of Beck et al. (2020).

The cost of global pancake collapse is given by frame volume times the failure cost multiplier:

$$C_{PG} = k_{brittle}C_{\text{const.}}(\lambda_B = 1, \lambda_C = 1) \quad (27)$$

Note that failure costs are computed w.r.t. the strengthened frame but for unitary design factors $\lambda_B = \lambda_C = 1$. This makes the optimization problem more stable, according to our experience (Beck et al. 2019; Beck 2020). This can be justified as damage to building contents, lost revenue, and costs of compensation are one order of magnitude higher than structural material costs (as reflected by $k \geq 40$).

Eq. (27) is also the collapse failure cost under normal loading conditions: since the frame is regular, bending failure of one beam, or crushing failure of one column, under uniform loading conditions, represents the simultaneous failure of all beams and all columns. This is an obvious simplification, as it neglects the bay-to-bay and story-to-story variations in loading and in member strengths that are observed in practice.

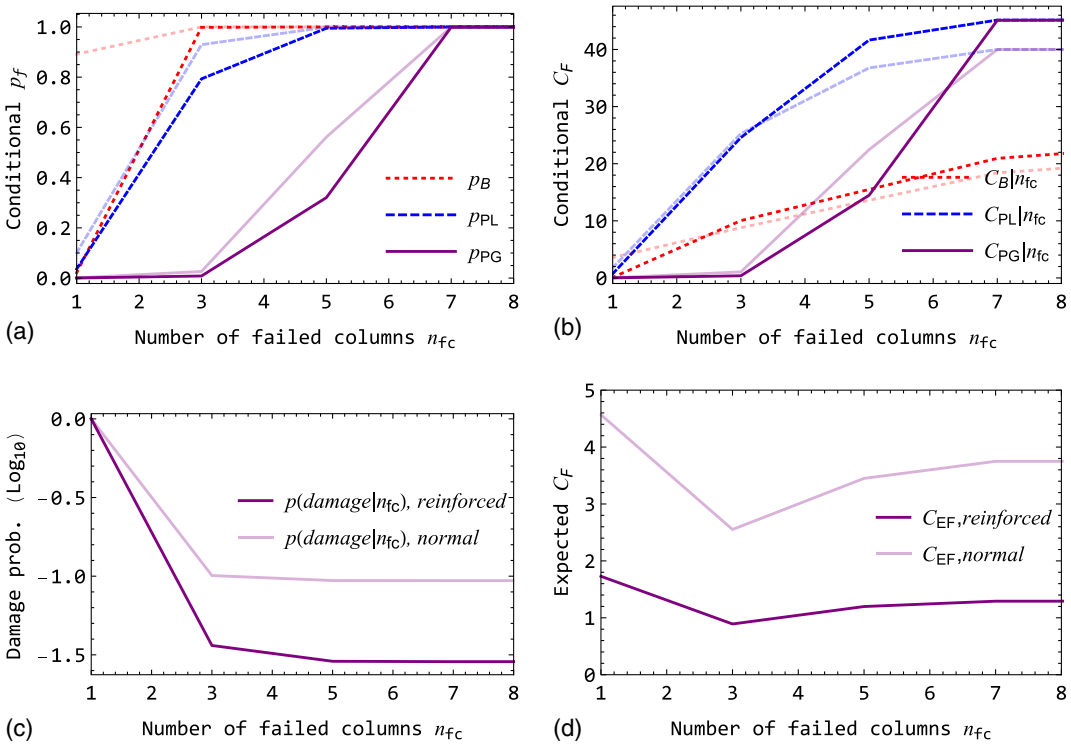

Fig. 2. (a) Conditional failure probabilities; (b) conditional costs of failure; (c) progressive damage probability; and (d) expected costs of failure of *normal* (fading lines) and *strengthened* (strong lines) frames, in terms of the number of failed columns ($n_{f,c}$).

Progressive Collapse of the Regular Frame

If the frame suffers initial damage, leading to loss of $n^0_{r,c}$ columns and $n^0_{r,s}$ stories, progressive failure may occur. In the context of progressive failure, we refer to the number of failed columns ($n_{f,c}$), instead of the number of removed columns ($n_{r,c}$). Clearly, the role of these variables in the formulation is the same, and the initial number of failed columns is $n^0_{f,c} = n^0_{r,c}$. The chain of events that may follow initial damage includes

1. Bending failure of beams of the $n^0_{f,c}+1$ affected bays, which may propagate upwards affecting all floors, but is otherwise self-arresting,
2. Local crushing failure of two adjacent columns, which may propagate horizontally, affecting two additional bays, with $n_{f,c} = n^0_{f,c}+2$, and so on, until it is naturally arrested, or until complete (global pancake) collapse, and
3. Local crushing failure of $n_{f,c} = n^0_{f,c}+2$ columns may also cause the bending failure of $n^0_{f,c}+3$ bays, and so on.

The likelihood of occurrence of the presented progressive failure events is controlled by beam and column strengths, which depend on design factors λ_B and λ_C. The conditional probabilities of occurrence of local bending, local pancake, and global pancake collapse events are given as

$$p_B = \Phi[-\beta_B(\lambda_B, n_{f,c})], \qquad p_{PL} = \Phi[-\beta_{PL}(\lambda_C, n_{f,c})],$$
$$p_{PG} = \Phi[-\beta_{PG}(\lambda_C, n_{f,c})] \tag{28}$$

In this problem, failure consequences are related to frame areas that overlap [see Fig. 2 in Masoero et al. (2013)]. For the same number of removed columns, the area affected by local pancake collapse includes the area affected by bending collapse. Progressive collapse due to local pancake, for $n_{f,c}+2$, encompasses the same area affected by local pancake with $n_{f,c}$ failed columns. Global pancake failure affects the whole frame. In this setting, a reasonable approximation to the failure tree is to consider the maximum expected cost among all possible failure events. This approximation is also possible because the failure modes are likely to be strongly correlated, as they depend on the same loads and initial damage event.

For the initial discretionary column removal event, the maximum expected cost becomes

$$Max[p_B C_B(n^0_{f,c}), p_{PL}C_{PL}(n^0_{f,c}), p_{PG}C_{PG}(n^0_{f,c})] \tag{29}$$

Note that $C_{PG} > C_{PL} > C_B$, but the presented terms are balanced by the corresponding probabilities, which depend on partial factors λ_B and λ_C.

Local pancake collapse, with the removal of $n^0_{f,c}$ columns, may evolve into bending collapse or progressive local pancake collapse, affecting $n^0_{f,c}+2$ columns, and so on. The conditional probability that local pancake collapse will advance, to involve $n_{f,c}+2$ columns, is given by $p_{PL}(n_{f,c}+2)$. The unconditional probability is: $p_{PL}(n_{f,c})p_{PL}(n_{f,c}+2)$. Thus, the expected collapse cost for progressive failure is given by

$$p_{PL}(n_{f,c})p_{PL}(n_{f,c}+2)Max[p_B C_B(n_{f,c}+2), C_{PL}(n_{f,c}+2),$$
$$p_{PG}C_{PG}(n_{f,c}+2)] \tag{30}$$

With these preliminaries, the total expected cost for progressive collapse failure of the regular 2D frame is given by

$$C_{TE}(\lambda_B, \lambda_C) = C_{const.}(\lambda_B, \lambda_C) \tag{a}$$
$$+C_{const.}(1,1)\Phi[-\beta^{50}_B(\lambda_B)] + C_{PG}\Phi[-\beta^{50}_{PG}(\lambda_C)] \tag{b}$$
$$+p_{LD}Max[p_B C_B(n^0_{f,c}), p_{PL}C_{PL}(n^0_{f,c}), p_{PG}C_{PG}(n^0_{f,c}), \tag{c}$$
$$\ldots Max^{(n_c-2)}_{j=(n^0_{f,c}+2)}\{p_{PL}(j-2)p_{PL}(j)Max[p_B C_B(j),$$
$$C_{PL}(j), p_{PG}C_{PG}(j)]\}] \tag{d}$$
$$\tag{31}$$

In Eq. (31), line (b) corresponds to the global failure of the intact frame under normal loading conditions. Line (c) corresponds to the maximum expected cost in the initial discretionary local damage event. Line (d) accounts for the maximum expected cost during the eventual progressive collapse. Note that the operator $Max[]$ in line (c) extends to line (d), i.e., only the event leading to maximum expected failure cost is computed. This warrants that the cost of collapse will not exceed $k_{brittle}C_{const.}(1,1)$. The counter j in line (d) should vary in steps of two units.

Objective Function for Cost-Benefit Optimization

The cost terms defined in the last section, and grouped in Eq. (31), already include the expected cost of failure of the intact structure (due to bending or global pancake collapse), the expected costs of progressive failure, and the expected costs of collapse. Hence, the risk-optimization problem in Eq. (3) is solved, considering the total expected costs in Eq. (31) as the objective function.

Results for the Reference Case

The formulation just presented was implemented in Mathematica 12. The optimization problem is solved using various built-in algorithms of function *Minimize* (Wolfram Research 2018). Results for the reference case are presented in this section.

Conditional Failure Probabilities, Conditional and Expected Costs of Failure

We start by illustrating the conditional failure probabilities in Eq. (28), the conditional costs of failure in Eqs. (29) and (30), and the expected costs of failure in lines (b), (c), and (d) of Eq. (31).

Figs. 2(a–d) show conditional failure probabilities, conditional costs of failure, progressive damage probabilities, and expected costs of failure as the number of failed columns increases for the *reference* frame. The strong lines in these figures are the results for the *strengthened* frame, whereas the fading lines correspond to the *normal* frame (normal loading conditions). As expected, the response of the strengthened frame, given initial damage, is better: failure probabilities are smaller for all failure modes [Fig. 2(a)], and expected costs of failure are significantly smaller [Fig. 2(d)].

In Fig. 2(a), we observe that conditional failure probabilities are very large for the normal frame, especially in bending. For the strengthened frame, conditional failure probabilities start smaller but increase rapidly as the number of failed columns increases from one to three. The conditional probability of global pancake failure is small up until $n_{f,c} = 3$ and increases rapidly for $n_{f,c} > 3$. Conditional costs of failure [Fig. 2(b)] are larger for the *normal* frame for the initial number of removed columns ($n^0_{r,c} = 1$). However, as the number of failed columns increases, these conditional cost terms become larger for the strengthened frame since the total cost of the strengthened frame is larger than the total cost of the normal frame. Damage probabilities [Fig. 2(c)] start at $p[LD|n_{f,c}] = 1$ for $n_{f,c} = 1$, but they drop faster for the strengthened frame as $n_{f,c}$ increases. Two opposing factors explain the V-shapes in expected costs of failure [Fig. 2(d)]: as the number of failed columns increase, the damage area increases, but the event probabilities decrease. As a result, we see that expected damage for the strengthened frame reaches a plateau that is much lower than the expected damage for the normal frame.

The conditional probabilities and cost terms illustrated in Fig. 2 are basically the same terms of the robustness index recently proposed by Praxedes et al. (2021).

Optimal Design of the Reference Frame

By solving the cost-benefit optimization problem in Eq. (3) for $p_{LD} = 0.1$, the optimal design values $\lambda^*_B = 0.9$ and $\lambda^*_C = 1.3$ are found. Hence, the optimizer reduces the strength of beams, and increases the strength of columns, in comparison to the strengthening resulting from Eqs. (11) and (12). Conditional failure probabilities, conditional costs of failure, local damage probabilities, and expected costs of failure of the *optimally strengthened* frame are compared with the *strengthened* frame in Figs. 3(a–d).

As observed in Fig. 3(a), by reducing λ_B, the optimizer increases conditional bending failure probabilities for one and two lost columns. At the same time, the optimal solution reduces the conditional local pancake probabilities for up to five lost columns. Global pancake collapse probability is reduced between three and six lost columns. Fig. 3(b) shows that the conditional cost of bending failure is not affected by the slight increase in conditional bending failure probabilities. Yet, the conditional costs of local and global pancake collapse are reduced for the optimally strengthened frame. The changes observed in Figs. 3(a and b) are not very large, but they are significant in terms of reducing the probability of damage propagation [Fig. 3(c)] and the total expected costs of failure [Fig. 3(d)]. Hence, the risk-optimization results in a better balance between the failure modes and the corresponding expected costs of failure.

Results for Other Frame Configurations

Problem Variants

Several problem variants are considered in the sequence. This includes frames of different aspect ratios (number of stories × number of bays), as detailed in Table 3, as well as the aspect ratio of the individual bays, failure cost multipliers, strengthening costs, and size of the initial damage (Table 4). Table 3 includes a tall frame with 16 stories and 4 bays, the reference "square" frame with 8 stories and 8 bays, a low frame 4 stories height with 16 bays, as well as intermediate cases, all with similar "tributary" areas. In the sequence, the seven frame variations detailed in Table 3 are combined with the variations listed in Table 4. Further details about Table 4 variations are discussed with the results.

Optimal Safety Factors versus Local Damage Probability

Fig. 4 shows the optimal design factors λ^*_B and λ^*_C for tall and low buildings (Table 3) as a function of local damage probability (p_{LD}). Fig. 5 shows corresponding optimal values of bending and pancake reliability indexes, also for tall and low frames. Results for the *reference* frame follow the same pattern and would be situated between those of the tall and the low frames in Figs. 4 and 5. As can be observed, optimal reliability indexes (Fig. 5) follow the same overall trend of the optimal design factors (Fig. 4), although the relationship between them is not linear. Note that $\lambda_C = 0.85/0.65 = 1.3$ corresponds approximately to current design practice for RC columns.

As observed in Fig. 4, optimal design factors change significantly with the probability of initial damage; the only exception is the column design factor, which is indifferent to p_{LD} for the low frame. For the tall frame, optimal values of λ^*_C are as high as 1.6 for $p_{LD} = 1$, dropping to around 1.2 for smaller p_{LD}. Clearly, for tall frames with a smaller number of columns, the loss of a single column has a much greater impact. Interestingly, for small p_{LD}, optimal λ^*_C's for tall frames is smaller than for low frames, a result that may be counterintuitive at first sight. However, note that the overload or strengthening factor for adjacent columns, given the

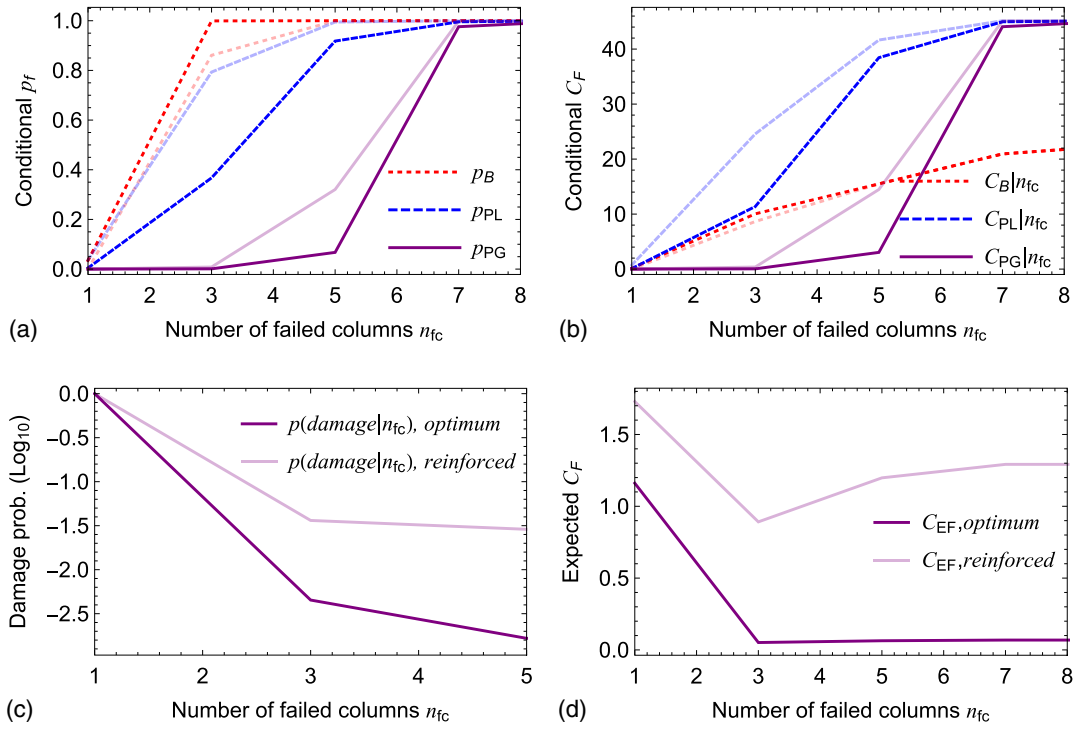

Fig. 3. (a) Conditional failure probabilities; (b) conditional costs of failure; (c) progressive damage probability; and (d) expected costs of failure of *strengthened* (fading lines, $\lambda_B = \lambda_C = 1$) and *optimally strengthened* (strong lines, λ_B^* and λ_C^*) frames, in terms of the number of failed columns ($n_{f,c}$).

Table 3. Variants of aspect ratio (number of stories × bays)

Aspect ratio variations	Number of stories × bays $(n_s \times (n_c - 1))$	Area
Tall frame	(16×4)	64
Intermediate	(13×5)	65
Intermediate	(11×6)	66
Reference case: "square" frame	(8×8)	64
Intermediate	(6×11)	66
Intermediate	(5×13)	65
Low frame	(4×16)	64

Table 4. Other problem variants

Set	Problem variants	Case
1	Aspect ratio of individual bays	$L = 2H$ *reference case* $L = H$ with half the tributary area $L = 2H$ by doubling the number of columns (n_c) $L = 3H$ with 50% increase of tributary area
2	Cost multipliers	$k_{ductile} = 20$, $k_{brittle} = 40$ different cost multipliers, *reference case* $k_{ductile} = k_{brittle} = 40$ same cost multipliers for ductile and brittle failures $k_{ductile} = 40$, $k_{brittle} = 80$ different cost multipliers, increased $k_{ductile} = 50$, $k_{brittle} = 200$ different cost multipliers, increased proportion
3	Strengthening cost	$\alpha_B = \alpha_C = 0.7$ *reference case* $\alpha_B = \alpha_C = 0.9$ higher cost of strengthening $\alpha_B = 0.5$, $\alpha_C = 0.9$ different costs of strengthening for beams/columns $\alpha_B = \alpha_C = 0.7$, but all stories are strengthened ($n_{reinf,s} = n_s$)
4	Extent of initial damage	$(n_{r,c}^0 \times n_{r,s}^0) = (1 \times 1)$ *reference case* $(n_{r,c}^0 \times n_{r,s}^0) = (1 \times 0)$ reduced extent of initial damage $(n_{r,c}^0 \times n_{r,s}^0) = (2 \times 1)$ increased extent of initial damage $(n_{r,c}^0 \times n_{r,s}^0) = (3 \times 2)$ largest extent of initial damage

loss of a single column, is $R_{sf} = 1.0$ for the low frame, but $R_{sf} = 1.38$ for the tall frame (Table 5). Hence, it is cheaper to strengthen columns of the low frame, as the additional design margin is (only) $\lambda_C^* \approx 1.4$ for these columns. For the tall frame, the cost of strengthening adjacent columns is proportional to $1.6 \times 1.38 = 2.2$, for $p_{LD} = 1$, dropping to around $1.2 \times 1.38 = 1.67$ for smaller p_{LD}. It is also relevant that for low frames, global pancake failure is unlikely for a single column failure; yet, the whole frame may collapse if local pancake failure progresses horizontally (this could also be avoided by structural fuses, which is not addressed herein). Hence, it is relatively cheaper to protect the low frame against progressive local pancake failure. For the tall frames, the loss of a single column has a greater impact on local and global pancake failure probabilities, as observed in Fig. 5.

Optimal design factors for bending are larger than one for tall frames and $p_{LD} \gtrsim 0.1$, and smaller than one otherwise. Optimal λ_B^*'s are significantly larger for tall buildings, because bending failures due to column loss propagate upwards, causing greater

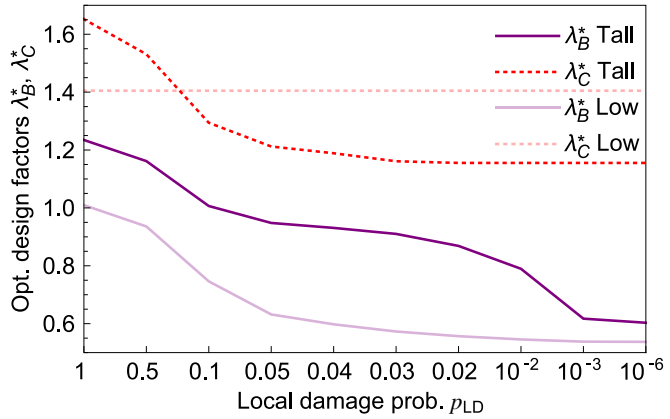

Fig. 4. Optimal design factors λ_B^* and λ_C^* as a function of local damage probability (nonlinear horizontal scale).

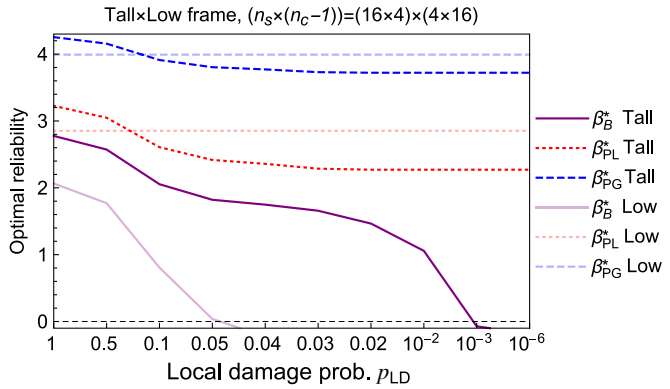

Fig. 5. Optimal reliability indexes for bending (β_B^*), local (β_{PL}^*), and global pancake (β_{PG}^*), as a function of local damage probability (nonlinear horizontal scale).

Table 5. Strengthening factors for beams (B_{sf}) and columns (R_{sf}) for different frames and extents of initial damage [Eq. (13)]

Frame	Factor	Initial damage $(n_{r,c}^0 \times n_{r,s}^0)$			
$(n_s \times (n_c - 1))$	(1×1)	(1×0)	(2×1)	(3×2)	
(16×4)	R_{sf}	1.38	1.42	1.98	2.47
(13×5)	R_{sf}	1.29	1.34	1.87	2.29
(11×6)	R_{sf}	1.24	1.29	1.78	2.17
(8×8)	R_{sf}	1.15	1.23	1.66	1.95
(6×11)	R_{sf}	1.08	1.17	1.55	1.74
(5×13)	R_{sf}	1.04	1.15	1.48	1.60
(4×16)	R_{sf}	1.00	1.13	1.40	1.40
All	B_{sf}	2.06	2.06	4.13	6.19

consequences for taller buildings. Optimal design factors for bending become significantly smaller as p_{LD} is reduced. Very small values of λ_B^* do not have practical significance, as minimal required beam strength would likely be determined by serviceability (displacement) limit states. Comparing Figs. 4 and 5, it can be observed that when λ_B^* drops to about 0.6, the optimal bending reliability index β_B^* drops to zero. As argued in Beck et al. (2020), this corresponds to an optimal design that is indifferent to the objective consideration of discretionary column removal. This is detailed in the sequence.

Threshold Local Damage Probabilities

As illustrated in Figs. 4 and 5, the probability that a regular frame suffers local damage, leading to the loss of one column and two beams of a single floor, has a significant impact on the optimal structural design. As p_{LD} becomes smaller, the optimal design changes from an alternative load path, or load bridging design, with large design factors, to an alternative path design with minimal design factors, which eventually approaches the usual design (with no discretionary element removals). This becomes a smooth transition because the formulation proposed in Beck et al. (2020) and employed herein [Eq. (3)] combines normal and abnormal loading conditions in the same objective function [Eq. (31)].

As argued by Beck et al. (2020, 2021), a threshold local damage probability (p_{LD}^{th}) can be identified, above which design or strengthening considering discretionary element removals has better cost-benefit than design under normal loading conditions. Two different situations have to be acknowledged in this context: (A) design and strengthening considering current normative (with $\lambda_B = \lambda_C = 1$); and (B) designs resulting from risk optimization [Eqs. (3) and (31)], with optimal values λ_B^* and λ_C^*. The resulting p_{LD}^{th}'s are conceptually the same but numerically different.

When current normative is considered (situation A), threshold local damage probabilities (p_{LD}^{th}) are identified by comparing total expected costs for usual design [Eqs. (9) and (10)], and for design/strengthening considering discretionary element removals [Eqs. (11) and (12) with $\lambda_B = \lambda_C = 1$]. This is illustrated in Figs. 4 and 7 of Beck et al. (2020) and in Figs. 4, 7, and 8 of Beck et al. (2021). This agrees with the practical definition presented in Beck et al. (2020) and reproduced in the introduction. In this paper, we address a variety of frames, with different aspect ratios, different initial damages, and different strengthening measures. For some of the taller frames, conventional progressive collapse design with $\lambda_B = \lambda_C = 1$ is always cheaper than the design under normal loading conditions. For some of the lower frames, the opposite is true. For these cases, it is impossible to find a root of the difference between total expected costs; hence, the most practical interpretation of p_{LD}^{th} cannot be employed.

For the risk-optimization problem, the threshold local damage probability (p_{LD}^{th}) is a point of indifference of the optimal solution, where two local minima with similar objective function values are observed: one is an alternative path solution with reduced optimal design margin for bending failure ($\lambda_B^* < 1$); the other is a solution with $\lambda_B^* \ll 1$, which approaches the design under normal loading conditions. These local minima solutions are illustrated in Figs. 3, 8, 9, and 13–16 of Beck et al. (2020) and in Figs. 3 and 9 of Beck et al. (2021). Local minima do not always exist, as seen in Fig. 6 of Beck et al. (2020). Automatic identification of local minima is difficult to implement.

The indifferent behavior, leading to local minima of similar total expected costs, is associated with a transition, from positive to negative, of the optimal reliability index for bending, β_B^*. This transition is illustrated in Fig. 5 and Table 5 of Beck et al. (2020), in Fig. 5 of Beck et al. (2021), and can also be observed in Fig. 5 for the tall and low frames considered herein. Hence, a practical way of identifying the indifferent design is by finding the p_{LD} root for which the optimal bending reliability index β_B^* is zero. This approach is adopted in this paper. The *Solve* function of Mathematica (Wolfram Research 2018) is used for root finding. As can be observed in Fig. 5, for the low frame, $p_{LD}^{th} \approx 0.05$, and for the tall frame, $p_{LD}^{th} \approx 10^{-3}$. Fig. 6 shows p_{LD}^{th} values for frames of different aspect ratio and following the problem variants in Tables 3 and 4.

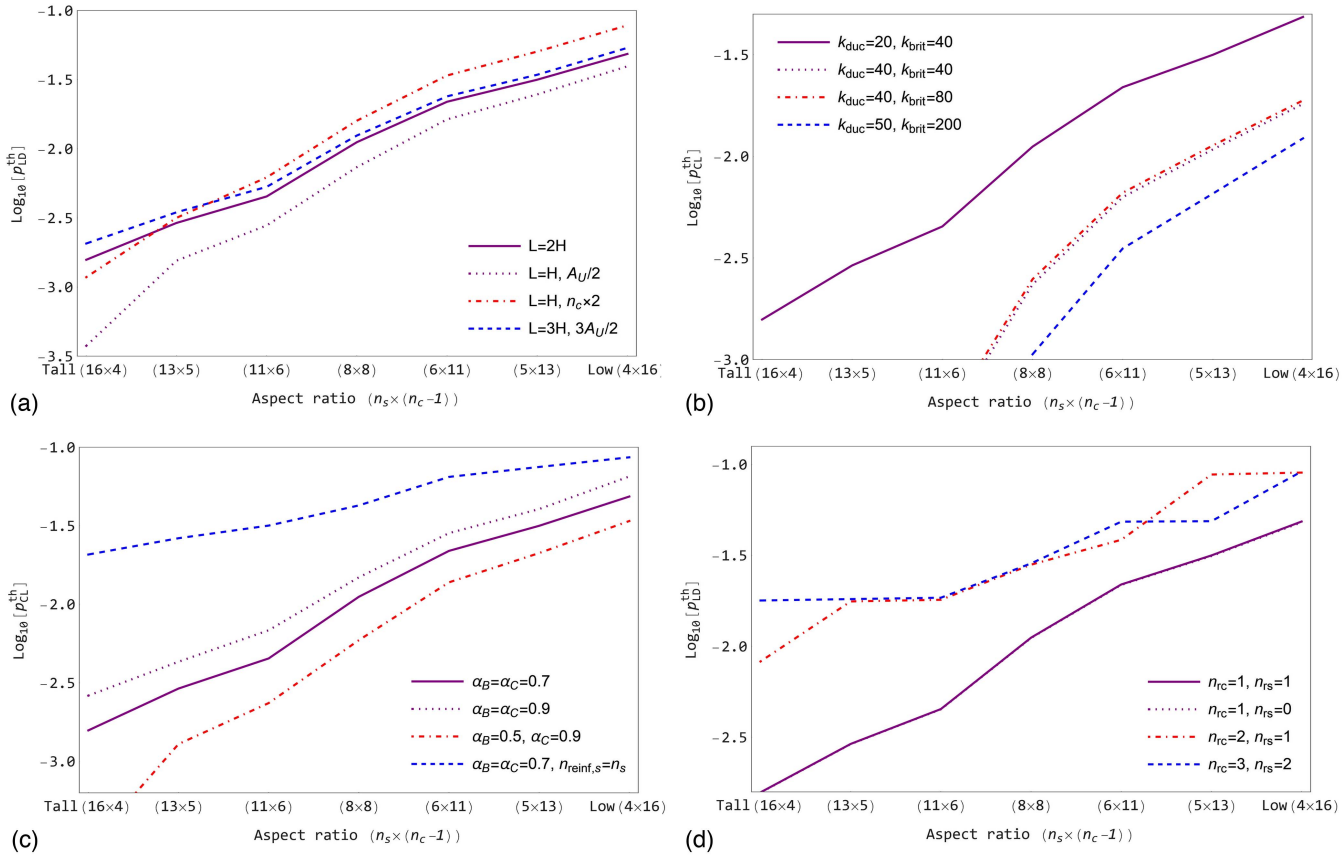

Fig. 6. Threshold local damage probability p_{LD}^{th}, as a function of (a) frame and bay aspect ratios; (b) failure cost multipliers; (c) costs of strengthening; and (d) extents of initial damage.

As observed in Fig. 6(a), lower frames require higher local damage probabilities to justify strengthening with discretionary element removal. For taller frames, the threshold p_{LD}^{th} values are smaller, dropping to about 10^{-4}. This corresponds to an annual threat probability of 2×10^{-6}, which is of the order of magnitude of usual threats (gas explosions or fire, with 10^{-6} to 10^{-5} occurrences per year). This shows that design considering discretionary element removals can be economically justified for taller frames in an extension to results presented in Beck et al. (2020).

To keep the numbers in Fig. 6 in perspective, Thöns and Stewart (2019) found that protective measures for iconic bridges are not economical for threat probabilities smaller than 10^{-4} per year, and Stewart (2017) found that strengthening buildings is only cost-effective for threat probabilities larger than 10^{-3} per building per year. These numbers correspond to 50-year local damage probabilities between $5 \times 10^{-3} \leq p_{LD}^{th} \leq 5 \times 10^{-2}$, well within the range of p_{LD}^{th} values in Fig. 6.

Results for Set 1: Effect of Frame and Bay Aspect Ratios

Threshold Probabilities

Fig. 6(a) also shows threshold local damage probability results for bays of different aspect ratios. The purple line is for the *reference* case, with $L = 2H$. When the bay length is reduced by half ($L = H$, dotted line), with a corresponding reduction in tributary area (A_U), p_{LD}^{th} values are reduced. When the bay length is increased by 50% ($L = 3H$, dashed blue line), with a corresponding increase in tributary area, p_D^{th} values are increased. Yet, if the bay length is reduced by half, by doubling the number of columns ($L = H$, dash-dotted red line), a different behavior is observed: p_{LD}^{th} values increase for lower frames but decrease for taller frames. Hence, we observe that the frame aspect ratio, as given by the number of stories × bays, or $(n_s \times (n_c - 1))$, has a greater impact on results than the actual aspect ratio of individual bays.

Optimal Design Factors and Reliability Indexes for $p_{LD} = 0.1$

As observed in Figs. 4 and 5, optimal design factors and reliability indexes vary significantly with the initial local damage probability. In the following, we analyze how these optimal values change for the frames of different aspect ratios by fixing $p_{LD} = 0.1$. Recall that this 50-year probability corresponds to an annual threat probability of 2.1×10^{-3}. This value is above usual threat probabilities for column loss in buildings but it is in the range for which progressive collapse design is cost-effective for all frames studied herein, as shown in Fig. 6.

Fig. 7 illustrates optimal design factors for beams (λ_B^*) and columns (λ_C^*) for all frame and bay aspect ratios considered herein. Optimal bending design factors are nearly unitary for tall frames and reduce continuously for lower frames. This matches the behavior observed in Fig. 4: larger design factors are justified for taller frames because bending failures would progress upwards. As frame height is reduced, the p_{LD}^{th} values observed in Fig. 6(a) get closer to the fixed $p_{LD} = 0.1$ of Fig. 7, this also explains why optimal λ_B^*'s are reduced. The smallest λ_B^*'s are obtained when the number of columns is doubled, in comparison to the *reference* case.

An interesting nonproportional effect is observed for the optimal column design factors. As frame height increases, optimal λ_C^*'s are reduced. This trend was observed in Fig. 4: for lower frames,

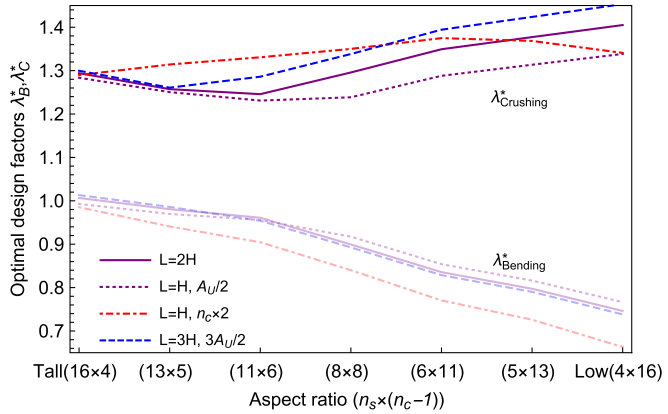

Fig. 7. Optimal design factors λ_B^* (fading lines) and λ_C^* (strong lines), as a function of frame and bay aspect ratios, for $p_{LD} = 0.1$.

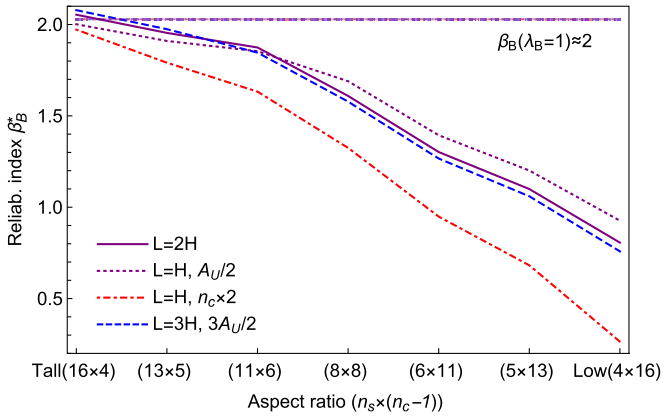

Fig. 8. Optimal reliability indexes for bending (β_B^*), for $p_{LD} = 0.1$.

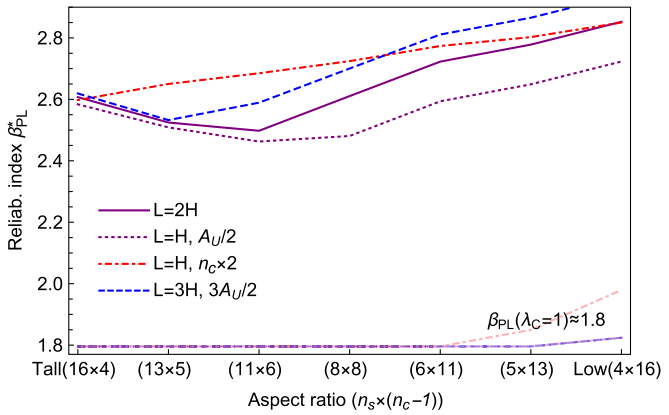

Fig. 9. Optimal reliability indexes for local pancake (β_{PL}^*), for $p_{LD} = 0.1$.

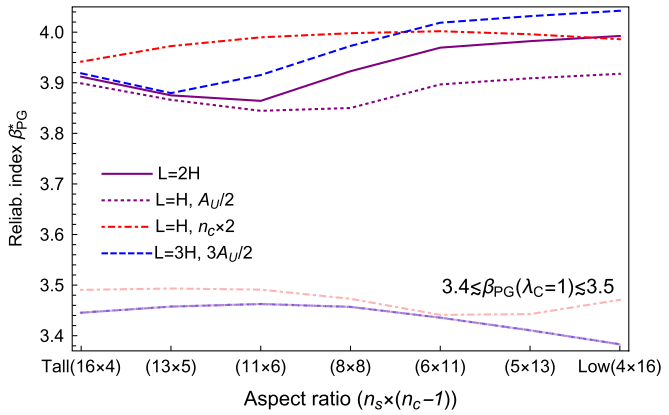

Fig. 10. Optimal reliability indexes for global pancake (β_{PG}^*), for $p_{LD} = 0.1$.

the column strengthening factor R_{sf} is small, and the importance of avoiding (progressive) local pancake failures is large. Yet, for the three taller frames in Fig. 7, this tendency is reverted, and optimal λ_C^*'s increase. This may be to avoid global pancake failures. Optimal λ_C^*'s for frames with a doubled number of columns show a distinct, more indifferent behavior.

By looking at the joint behavior of λ_B^*'s and λ_C^*'s and not considering the case with additional columns (dash-dotted red line), it is observed that for frames lower than (11×6), reductions of λ_B^*'s are accompanied by increases in λ_C^*. As the frames become lower and wider, the consequences of beam failures are reduced (upward progression), but the consequences of local pancake failures increase (horizontal progression). For frames taller than (11×6), this tendency changes, and both optimal design factors increase with increased frame height (and reduction in the number of columns). This occurs because the consequences of beam and column failures increase with frame height. Hence, what we observe in Fig. 7 is a competition between beam bending and column crushing failure modes. The resources allocated into frame strengthening need to be compensated by reductions in expected costs of failure. The optimal allocation of these resources between beams and columns changes according to the frame and bay aspect ratios, as observed in Fig. 7. Actual values of optimal design factors in Fig. 7 are valid for this paper only, but the identified trends should be valid for real structures as well.

Figs. 8–10 illustrate the optimal bending, local pancake, and global pancake reliability indexes, respectively. Overall, the trends observed in Fig. 7 can be identified in Figs. 8–10. The fading lines in Figs. 8–10 illustrate reliability indexes obtained for the usual progressive collapse design, with $\lambda_B = \lambda_C = 1$. For bending (Fig. 8), the usual design leads to constant β_B's around $\beta_B = 2$, whereas optimal design has a large impact on bending failure probabilities. For local pancake (Fig. 9) and global pancake (Fig. 10), the usual progressive collapse design leads to nearly constant collapse probabilities. These are significantly reduced by optimal design. Overall, it is observed in Figs. 8–10 that optimal design finds a better balance between the different failure modes of the regular frame subject to loss of load-bearing elements.

Results for Set 2: Effect of Cost Multipliers

It is expected that results of risk optimization depend, to a great extent, on failure cost multipliers k. Consequences of failure will vary significantly with building use and occupancy, as well as the surrounding environment. Fig. 6(b) illustrates threshold local damage probabilities p_{LD}^{th} for different failure cost multipliers. The continuous purple line is the result for the *reference* case, with $k_{brittle} = 2k_{ductile} = 40$. As observed, increased failure consequences lead to a drop in p_{LD}^{th} values, making strengthening for load bridging cost-effective for a greater range of frame structures. Changes in k_{ductile} have a greater impact on p_{LD}^{th}, as this value is

determined directly from the root $\beta_B^* = 0$ (ductile failure of beams is assumed). A doubling of $k_{brittle}$, for fixed k_{ductile}, produced a minor impact on results (dotted and dash-dotted lines). Results for optimal design factors and reliability indexes are similar to those shown in Figs. 7–10 in terms of relative trends. Overall, for larger cost multipliers, hence larger consequences of failure, optimal design factors, and reliability indexes are larger. Optimal λ_B^*'s increase with $k_{ductile}$, and optimal λ_C^*'s increase with $k_{brittle}$.

Results for Set 3: Effect of Strengthening Cost

In Beck et al. (2020), it was shown for a single frame of 11 bays by 11 stories that the decision to strengthen a structure for load bridging over failed load-bearing elements depends on strengthening costs. As discussed in the "Construction Cost" section, strengthening costs depend on local costs of materials, both absolute and relative. Strengthening costs also depend strongly on the strengthening decisions, for instance, the decision on the number of stories and bays to reinforce. Herein, the default strengthening decision involves all columns and all beams of the first two floors ($n_{reinf,s} = 2$). Herein, we investigate the effects of strengthening costs on the optimal design of a wider range of frames.

Fig. 6(c) illustrates local damage probability thresholds, p_{LD}^{th}, for different participation factors α_B and α_C. Recall that α_B is the participation of cost of steel in strengthening RC beams: doubling the plastic hinge strength of beams requires doubling the amount of steel (approximately), and this would lead to a $2\alpha_B$ impact on the cost of strengthened beams. The continuous purple line in Fig. 6(c) is the *reference* case, with $\alpha_B = \alpha_C = 0.7$, and $n_{reinf,s} = 2$. When the cost participation factors increase to $\alpha_B = \alpha_C = 0.9$, threshold p_{LD}^{th} values increase for all frames, making progressive design cost-effective only for larger threat probabilities. If α_B is reduced to $\alpha_B = 0.5$, with $\alpha_C = 0.9$, we observe that the impact of α_B reduction is larger than the impact of α_C increase (from 0.7). This is a direct consequence of evaluating p_{LD}^{th} from the root $\beta_B^* = 0$. If participation factors are maintained at $\alpha_B = \alpha_C = 0.7$ but the decision is to reinforce the whole frame, p_{LD}^{th} increases significantly for all frames. Hence, since the strengthening decision has a greater impact on construction costs, it is justified only for larger threat probabilities. The threat probabilities that justify strengthening the whole frame are significantly larger than usual values for gas explosion or fire threats.

Fig. 11 illustrates the optimal safety factors for beam bending and column crushing in terms of the strengthening cost factors. The optimal λ_B^*'s vary in proportion to the beam cost participation factor α_B, with larger λ_B^*'s obtained for smaller α_B. Similar behavior is observed when α_C is increased: increasing α_C leads to a reduction in λ_C^*'s. When the relative value of cost factors changes, an unexpected behavior is observed: reducing α_B while keeping α_C constant produced a reduction in optimal λ_C^*'s for lower frames but an increase in λ_C^*'s for taller frames. For taller frames, the reduction in beam strengthening cost led to an increase in optimal λ_B^*'s but also to an increase in optimal λ_C^*'s! This confirms the competition between failure modes, observed in Fig. 7: for tall frames, stronger beams need to the accompanied by stronger columns in order to avoid pancake failures. The dash-dotted red line in Fig. 11 shows that the competition between failure modes is affected by the relative value of cost factors for strengthening beams and columns.

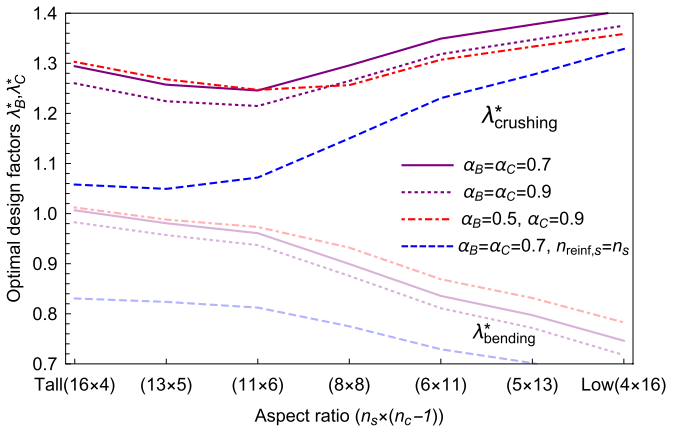

Fig. 11. Optimal design factors λ_B^* (fading lines) and λ_C^* (strong lines), as a function of frame aspect ratio, for different costs of strengthening and $p_{LD} = 0.1$.

Results for Set 4: Effect of Extent of Initial Damage

One of the largest unknowns in alternative path (APM) design is the extent of initial damage, for which alternative load paths should be developed. This uncertainty relates to the actual response of the structure, given unknown initial damage, but also to the discretionary element removal scenarios for which APM strengthening is performed. To simplify matters, in this paper, a match is considered between the design and the actual initial damage scenario. Mismatches should be addressed in future research.

Clearly, strengthening frames to sustain larger initial damage has an impact on construction costs. Table 5 shows the factors required for strengthening beams and columns to sustain the initial damages listed in Set 4 of Table 4 (and in the header of Table 5). For the beams to sustain loss of 1, 2 and 3 columns requires plastic hinge strengths that are about 2×, 4×, and 6× larger than the strength under normal loading conditions. The strengthening factor for columns varies significantly with frame height, as shown in Table 5.

Fig. 6(d) shows how the local damage probability thresholds, p_{LD}^{th}, changes for different extents of initial damage. The *reference* case, with $(n_{r,c}^0 \times n_{r,s}^0) = (1 \times 1)$, is shown as a continuous purple line. As observed, a reduction in the number of affected beams ($n_{r,s}^0 = 0$) has no impact on p_{LD}^{th} (lines are superimposed). Yet, increasing the number of removed columns ($n_{r,c}^0$) has a large impact, making APM design economical only for larger threat probabilities. Typically, the probability of initial damage is inversely proportional to the extent of initial damage. A comprehensive analysis would require addressing conditional probabilities of progressive collapse given one, two, or more removed columns. This will be addressed in future research. Fig. 6(d) shows an intermingling effect of the results for two and three columns removed; this also deserves further investigation.

Fig. 12 illustrates the optimal safety factors for beam bending and column crushing in terms of the extent of initial damage. As observed, the initial damage has a larger impact on the optimal design factors for columns. Although load bridging over a larger span has a significant impact on beam strengthening factors (B_{sf} in Table 5), this does not reflect in large changes in optimal λ_B^*'s.

The competition between failure modes is also significantly affected by the extent of initial damage. The opposing trend between optimal λ_B^*'s and λ_C^*'s, which in Fig. 11 was observed for frames lower than (11×6), is now observed only for the two lowest frames (right in Fig. 12). With larger initial damage ($n_{r,c}^0 = 2$ or 3), the increase in λ_B^* for taller frames is accompanied by an increase in λ_C^*. For the larger extent of damage, strengthening beams makes pancake failures more likely. To avoid this, beams and columns need to be strengthened simultaneously.

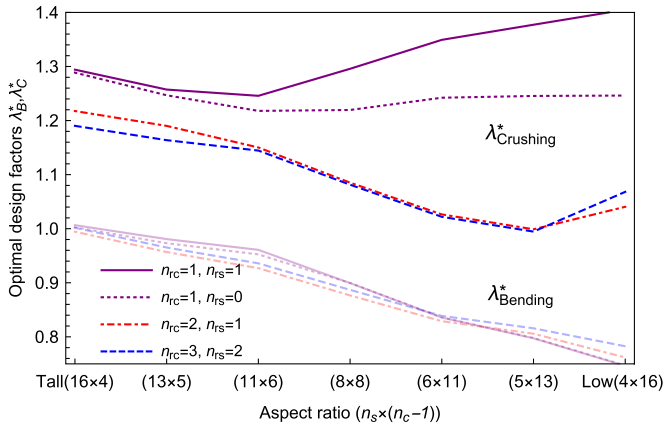

Fig. 12. Optimal design factors λ_B^* (fading lines) and λ_C^* (strong lines), as a function of frame aspect ratio, for different extents of initial damage and $p_{LD} = 0.1$.

Effects of Catenary Action

Catenary action provides significant additional strength to beams in progressive collapse. So far in this paper, catenary effects have not been included mainly because catenary effects are not objectively considered when determining required beam strengths and dimensions.

Eqs. (4) and (5) provide the distributed loads that produce plastic hinge mechanisms in beams of intact and damaged frames. Following Masoero et al. (2013), axial catenary effects can be considered by adding the following terms to Eqs. (4) and (5)

$$q_u^{I,B,pl} = \frac{16B_y}{L^2}\left(1+\frac{\psi}{8}\right), \qquad \text{(intact frame)} \qquad (32)$$

$$q_c^{B,pl}(n_{r,c}) = \frac{4B_y}{L^2(n_{r,c})}\left(1+\frac{\psi}{4}\right), \qquad \text{(damaged frame)} \qquad (33)$$

where $0 \le \psi \le 4$ is a dimensionless parameter depending on the kinematics of the failure mechanism and the beam's slenderness (Masoero et al. 2013). In this section, we briefly investigate the effects of considering catenary actions in the optimal risk-based design of regular frames using $\psi = 2$.

The catenary limit states derived from Eqs. (32) and (33) correspond to the ultimate limit before complete beam/slab collapses, but substantial (irrecoverable) building damage can be expected before this limit is reached. For the reference frame case considered in the "Results for the Reference Case" section, reliability indexes corresponding to the "catenary" limit states are shown in Table 2. As observed, catenary effects lead to higher beam reliability indexes. For the damaged condition, in particular, β^{apt} shows a significant increase from 2.03 to 3.36. In the risk optimization, this represents a reduced likelihood of ultimate beam collapse; yet, since significant building damage is expected for beam plastic hinge failures, we understand catenary action does not need to be considered in the optimization, as reported in previous sections. This is also a justification for considering larger failure cost multipliers for column failures in comparison to beam failures.

For completeness, we briefly report what happens when the additional beam strength, provided by catenary action, is considered in the risk-based optimization. Briefly, optimal design factors for beams, reported in Figs. 4, 7, 11, and 12, become significantly smaller, mostly smaller than 0.5. This clearly has no practical significance, as minimal beam strength would most certainly be determined by serviceability (displacement) limit states. Moreover, threshold columns loss probabilities determined as "zero-crossings" of the catenary beam reliability indexes go asymptotically to zero (when compared with Fig. 6). Loosely, this means that beam strengthening to produce catenary action has a positive cost-benefit for any initial damage probability; an observation that matches practical design recommendations.

Concluding Remarks

In this paper, we addressed the optimal design of regular frame structures subject to local damage due to abnormal events, leading to the loss of beams and columns. We employed a risk-based formulation that balances the costs of strengthening with the expected costs of progressive failure. We employed a simple analytical mechanical model where beams fail by plastic hinge mechanisms and columns fail by crushing under compressive loads. The model is limited to gravitational loads.

The analysis covered regular RC frames of different aspect ratios, failure consequences, cost of strengthening, and extent of initial damage. Results show that the economic benefit of strengthening frames to bridge over failed load-bearing elements (alternative path method or APM) is strongly dependent on threat probabilities. However, threshold local damage probabilities, above which APM design is justified, also depend strongly on frame aspect ratio, consequences of progressive collapse, and cost and reach of the strengthening measures. Typically, APM design is justified for larger threats, taller frames, larger progressive collapse consequences, cheaper strengthening, and limited strengthening measures. Typically, only targeted strengthening actions are cost-effective.

The analysis of optimal design factors for beams and columns and of frames of different aspect ratios revealed that local bending, local pancake, and global pancake failure modes "compete" for the strengthening resources. These resources need to be compensated by effective reductions in expected costs of failure. The optimal allocation of strengthening between beams and columns changes according to the frame aspect ratio. For lower frames, smaller design margins for beam bending are accompanied by larger margins against column crushing since bending failures progress upwards, whereas local pancake progresses horizontally. For taller frames and for greater initial damage, stronger beams need to the accompanied by stronger columns in order to avoid local and global pancake failures.

Results presented herein were obtained for simple mechanical modeling but provide useful insight for the optimal cost-benefit analysis and design of realistic structures.

Data Availability Statement

The Mathematica algorithms and routines used to obtain results presented in this paper will be made available upon reasonable request.

Acknowledgments

Funding of this research project by Brazilian agencies CAPES (Brazilian Higher Education Council), CNPq (Brazilian National Council for Research, Grant No. 309107/2020-2), and joint FAPESP-ANID (São Paulo State Foundation for Research—Chilean National Agency for Research and Development, Grant

No. 2019/13080-9) is also acknowledged. Valuable comments by the anonymous reviewers are also cheerfully acknowledged.

References

Adam, J. M., F. Parisi, J. Sagaseta, and X. Lu. 2018. "Research and practice on progressive collapse and robustness of building structures in the 21st century." *Eng. Struct.* 173 (Oct): 122–149. https://doi.org/10.1016/j.engstruct.2018.06.082.

Ang, A. H.-S., and W. H. Tang. 2006. *Probability concepts in engineering*. 2nd ed. New York: Wiley.

ASCE. 2016. *Minimum design loads for buildings and other structures*. ASCE 7. Reston, VA: ASCE.

ASCE. 2017. *Seismic evaluation and retrofit of existing buildings*. ASCE 41. Reston, VA: ASCE.

Beck, A. T. 2020. "Optimal design of redundant structural systems: Fundamentals." *Eng. Struct.* 219 (Sep): 110542. https://doi.org/10.1016/j.engstruct.2020.110542.

Beck, A. T., L. da Rosa Ribeiro, and M. Valdebenito. 2020. "Risk-based cost-benefit analysis of frame structures considering progressive collapse under column removal scenarios." *Eng. Struct.* 225 (Dec): 111295. https://doi.org/10.1016/j.engstruct.2020.111295.

Beck, A. T., and W. J. de Santana Gomes. 2012. "A comparison of deterministic, reliability-based and risk-based structural optimization under uncertainty." *Probab. Eng. Mech.* 28 (Apr): 18–29. https://doi.org/10.1016/j.probengmech.2011.08.007.

Beck, A. T., W. J. S. Gomes, R. H. Lopez, and L. F. F. Miguel. 2015. "A comparison between robust and risk-based optimization under uncertainty." *Struct. Multidiscip. Optim.* 52 (3): 479–492. https://doi.org/10.1007/s00158-015-1253-9.

Beck, A. T., L. R. Ribeiro, and M. Valdebenito. 2021. "Cost-benefit analysis of design for progressive collapse under accidental or malevolent extreme events." In *Engineering for extremes: Decision-making in an uncertain world*, edited by M. G. Stewart and D. V. Rosowsky. New York: Springer.

Beck, A. T., R. K. Tessari, and H. M. Kroetz. 2019. "System reliability-based design optimization and risk-based optimization: A benchmark example considering progressive collapse." *Eng. Optim.* 51 (6): 1000–1012. https://doi.org/10.1080/0305215X.2018.1502760.

Boito, D., and M. Kripka. 2020. "Parametric study of reinforced concrete plane frames structures through optimization." *Rev. CIATEC* 12 (1): 51–60. https://doi.org/10.5335/ciatec.v12i1.10646.

DoD (Department of Defense). 2013. *Design of buildings to resist progressive collapse*. UFC 4–023–03. Washington, DC: DoD.

Ellingwood, B., and T. V. Galambos. 1982. "Probability-based criteria for structural design." *Struct. Saf.* 1 (1): 15–26. https://doi.org/10.1016/0167-4730(82)90012-1.

Ellingwood, B., T. V. Galambos, J. G. MacGregor, and C. A. Cornell. 1980. *Development of a probability-based load criterion for American National Standard A58*. NBS Special Publication 577. Gaithersburg, MD: National Bureau of Standards.

Ellingwood, B. R. 2006. "Mitigating risk from abnormal loads and progressive collapse." *J. Perform. Constr. Facil.* 20 (4): 315–323. https://doi.org/10.1061/(ASCE)0887-3828(2006)20:4(315).

Ellingwood, B. R. 2007. "Strategies for mitigating risk to buildings from abnormal load events." *Int. J. Risk Assess. Manage.* 7 (6–7): 828–845. https://doi.org/10.1504/IJRAM.2007.014662.

Ellingwood, B. R., and D. O. Dusenberry. 2005. "Building design for abnormal loads and progressive collapse." *Comput.-Aided Civ. Infrastruct. Eng.* 20 (3): 194–205. https://doi.org/10.1111/j.1467-8667.2005.00387.x.

Gerasimidis, S., and J. Sideri. 2016. "A new partial-distributed damage method for progressive collapse analysis of steel frames." *J. Constr. Steel Res.* 119 (Mar): 233–245. https://doi.org/10.1016/j.jcsr.2015.12.012.

GSA (General Services Administration). 2013. *Alternate path analysis and design guidelines for progressive collapse resistance*. Washington, DC: GSA.

He, X.-H.-C., X.-X. Yuan, and W.-J. Yi. 2019. "Irregularity index for quick identification of worst column removal scenarios of RC frame structures." *Eng. Struct.* 178 (Jan): 191–205. https://doi.org/10.1016/j.engstruct.2018.10.026.

Hewitt, C. 2003. *Understanding terrorism in America: From the Klan to al Qaeda*, 106. New York: Routledge.

Marchand, K. E., and D. J. Stevens. 2015. "Progressive collapse criteria and design approaches improvement." *J. Perform. Constr. Facil.* 29 (5): B4015004. https://doi.org/10.1061/(ASCE)CF.1943-5509.0000706.

Masoero, E., P. Darò, and B. M. Chiaia. 2013. "Progressive collapse of 2D framed structures: An analytical model." *Eng. Struct.* 54 (Sep): 94–102. https://doi.org/10.1016/j.engstruct.2013.03.053.

Melchers, R. E., and A. T. Beck. 2018. *Structural reliability analysis and prediction*. 3rd ed. New York: Wiley.

Mueller, J., and M. G. Stewart. 2011. *Terror, security, and money: Balancing the risks, benefits, and costs of homeland security*. New York: Oxford University Press.

Nowak, A. S., A. M. Rakoczy, and E. K. Szeliga. 2011. "Revised statistical resistance models for R/C structural components." In *Proc., Andy Scanlon Symp. on Serviceability and Safety of Concrete Structures: From Research to Practice*. Farmington Hills, MI: American Concrete Institute.

Pantidis, P., and S. Gerasimidis. 2018. "Progressive collapse of 3D steel composite buildings under interior gravity column loss." *J. Constr. Steel Res.* 150 (Nov): 60–75. https://doi.org/10.1016/j.jcsr.2018.08.003.

Praxedes, C. 2020. "Robustness-based optimal progressive collapse design of RC frame structures." Ph.D. thesis, Dept. of Civil Engineering, Faculty of Engineering and Architectural Science, Ryerson Univ.

Praxedes, C., and X.-X. Yuan. 2021. "A novel robustness assessment methodology for reinforced concrete frames under progressive collapse threats." *J. Struct. Eng.* 147 (8): 04021119. https://doi.org/10.1061/(ASCE)ST.1943-541X.0003075.

Praxedes, C., and X.-X. Yuan. 2022. "Robustness-oriented optimal design for reinforced concrete frames considering the large uncertainty of progressive collapse threats." *Struct. Saf.* 94: 102139. https://doi.org/10.1016/j.strusafe.2021.102139.

Praxedes, C., X.-X. Yuan, and X.-H.-C. He. 2021. "A novel robustness index for progressive collapse analysis of structures considering the full risk spectrum of damage evolution." *Struct. Infrastruct. Eng.* https://doi.org/10.1080/15732479.2020.1851730.

SINAPI (Sistema Nacional de Pesquisa de Custos e Índices da Construção Civil). 2020. "Prices and costs in civil construction." [In Portuguese.] Accessed December 5, 2020. https://www.caixa.gov.br/poder-publico/modernizacao-gestao/sinapi/referencias-precos-insumos/Paginas/default.aspx.

Stewart, M. G. 2017. "Risk of progressive collapse of buildings from terrorist attacks: Are the benefits of protection worth the cost?" *J. Perform. Constr. Facil.* 31 (2): 04016093. https://doi.org/10.1061/(ASCE)CF.1943-5509.0000954.

Thöns, S., and M. G. Stewart. 2019. "On decision optimality of terrorism risk mitigation measures for iconic bridges." *Reliab. Eng. Syst. Saf.* 188 (Aug): 574–583. https://doi.org/10.1016/j.ress.2019.03.049.

Thöns, S., and M. G. Stewart. 2020. "On the cost-efficiency, significance and effectiveness of terrorism risk reduction strategies for buildings." *Struct. Saf.* 85 (Jul): 101957. https://doi.org/10.1016/j.strusafe.2020.101957.

Wolfram Research. 2018. *Wolfram Mathematica 11.3*. Documentation Center. Champaign, IL: Wolfram Research.